Differential Diagnosis of Gear and Bearing Faults

J. Antoni
Research Associate

R. B. Randall
Professor

School of Mechanical and Manufacturing Engineering,
The University of New South Wales,
Sydney 2052, Australia

This paper deals with the vibration-based diagnosis of rolling element bearings in the presence of strong interfering gear signals, such as is typical of helicopter gearboxes. The key idea consists in recognizing gear signals as purely periodic, whereas bearing signals experience some randomness and are close to cyclostationary, i.e. with a periodic bivariate autocorrelation function. This assertion is demonstrated by introducing a comprehensive model for the vibration generating process of bearing faults: distinctions are made between localized and distributed faults, between cyclostationary and pseudo-cyclostationary processes, and between additive and multiplicative interactions with gear signals. Finally, an original diagnostic procedure is proposed and its performance illustrated using simulated, experimental and actual cases. [DOI: 10.1115/1.1456906]

Introduction

Gears and rolling element bearings are critical elements in complex machinery to which predictive maintenance is often applied. The benefit of using vibration analysis for their monitoring and diagnosis has been demonstrated to be successful since the early 70's [1]. Since then, a number of *ad hoc* vibration-based techniques have been developed and perfected, and are nowadays well accepted. Some conventional established techniques for the diagnosis of gears include spectral analysis, cepstral analysis and demodulation analysis [2,3]. Techniques for the diagnostics of bearings include statistical analysis, spectral analysis, envelope analysis (High Frequency Resonance analysis), etc. [4,5]. These techniques work perfectly well for simple systems, where either the effects of the gears or bearings predominate over all other mechanisms, at least in some frequency range.

However, this may no longer be the case with more complex systems. In high-speed gearboxes, such as helicopter gearboxes, the gear-related vibrations extend into the high frequency range where also bearing faults manifest themselves, thus showing a mixture of the two types of signal over the whole frequency range. In the simplest case the mixture is found to be additive, but cases have been encountered where the bearing fault modulates the gear signal, due to the close physical connection of the gear and bearing elements. Under these circumstances, the *ad hoc* techniques for the diagnosis of gear or bearing signals are not guaranteed to apply any more.

This paper deals with the diagnostics of bearings in the presence of strong interfering gear signals, such as typically found in helicopter gearboxes. A strong emphasis is placed on how to distinguish between gear and bearing faults where the two signals may interact in a complex way, as in multiplicative mixtures. The key idea is based on recognizing gear signals as being purely periodic, whereas bearing signals experience some randomness and are approximately 2^{nd} order cyclostationary, i.e. with a periodic bivariate autocorrelation function.

One original contribution of this paper is to support the aforementioned assertion, by introducing a refined model for the vibration generating process of a bearing fault. From first principles, this model is shown to produce cyclostationarity or pseudo-cyclostationarity, under conditions which are discussed in detail. These results finally lead to the proposal of a new detection scheme, specifically dedicated to bearing faults in the presence of gear signals with which they are associated multiplicatively.

Contributed by the Technical Committee on Vibration and Sound for publication in the JOURNAL OF VIBRATION AND ACOUSTICS. Manuscript received September 2001; revised December 2001. Associate Editor: M. I. Friswell.

Vibration Signals Induced by Gears

The vibration signal arising from the operation of gears is typically modelled as a summation of phasors, each one related to a gearmesh frequency or one of its multiples. In turn, the amplitude and phase of each individual phasor is modulated by the shaft speeds. For a machine operating at constant speed, the resulting vibration signal is to a first approximation perfectly periodic, with a period which can actually be very long since all the shafts in the system share it. However a finite value always exists.

Typical faults affecting gears are pitting, spalls and, more seriously, cracks. It is believed that these faults, at least in their early stages, do not affect the periodic nature of the signal, because they contact periodically with exactly the same matching surfaces. Rather, only the strength and shape of the modulations are affected in a deterministic fashion. Indeed, this is the major assertion which makes cepstral techniques so powerful for detecting spalls, for example [2].

This assertion was verified in extensive experiments run on a test-rig in the Acoustics and Vibration Laboratories at the University of New South Wales (UNSW). The rig consists of a parallel shaft spur gear pair with interchangeable wheels, operating with a 1 to 1 ratio and which was equipped with accelerometers and a shaft encoder. One of the wheels had a simulated crack at the root of one tooth 5 mm$\times$0.5 mm across the whole width and generated by spark erosion. An example of a measured vibration signal is displayed in Fig. 1, along with the synchronous average taken over 25 cycles and the residual signal (signal with synchronous average removed) on the first cycle. Since the synchronous average captures all the periodic components in the signal, these figures clearly reveal that most of the energy in the signal was distributed over periodic components, despite the fault. Similar results were obtained over various sets of speeds and loads.

In practice, actual gear signals may experience some departure from exact periodicity due to speed fluctuations in the machine. If so, order tracking—resampling on an angular rather than a temporal basis—can be used to compensate for these variations.

Vibration Signals Induced by Bearings

The vibration signal arising from the operation of a rolling element bearing is not as straightforward as for gears. A distinction should be made between the signal coming from a bearing in good condition or from a faulty bearing. Our concern herein is only for the latter.

Most frequent rolling element bearing faults include damage of the inner race, the outer race and/or the rolling elements. Generally, during the early stages of the fault, the surface is only locally affected and vibrations are generated as a result of the repetitive impacts of the moving components on the defect. Therefore the

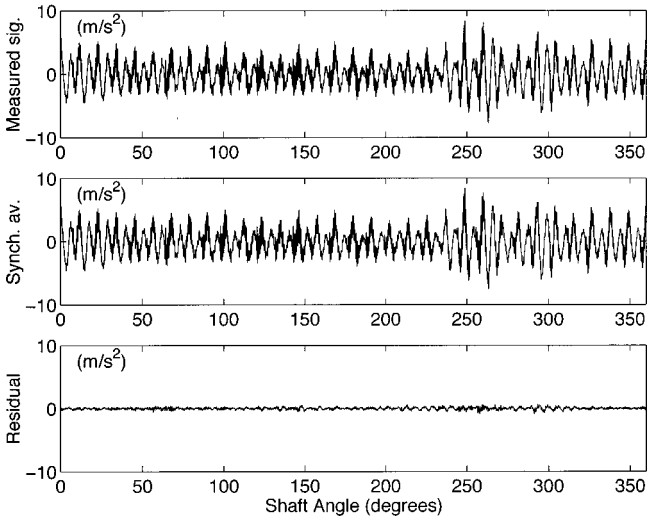

Fig. 1 Experiment on test-rig with a cracked tooth. (*a*) vibration signal (normalized amplitude) (*b*) synchronous average on 25 cycles (*c*) residual signal

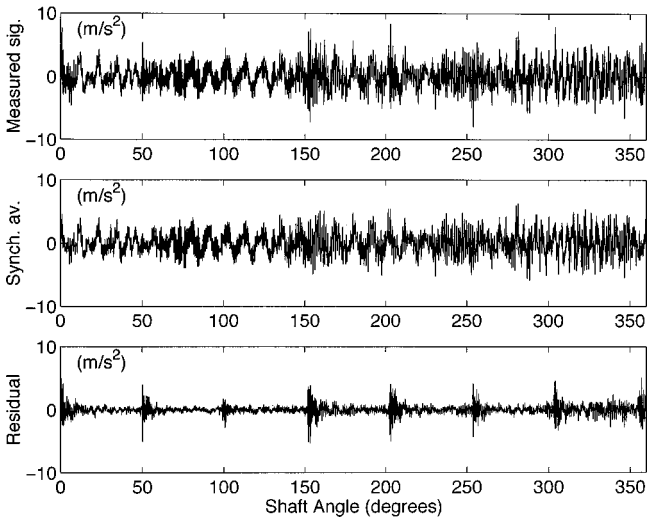

Fig. 2 Experiment on a test-rig with a faulty bearing (outer-race fault) (*a*) vibration signal (normalized amplitude) (*b*) synchronous average on 20 cycles (*c*) residual signal (signal with synchronous average removed)

overall vibration signal measured on the bearing is made up of a succession of oscillating bursts dominated by the major resonance frequencies of the structure. Moreover, depending on the location of the fault and the load distribution on the bearing, the whole pattern is further modulated either by the shaft speed (inner race fault), the cage speed (rolling element fault), or their difference (inner race fault with roller errors). The characteristic fault frequencies (rate of repetition of the bursts) and their modulations are well known, and their investigation is the basis of bearing diagnostics [5].

Actually, the rate of repetition and the amplitude of the bursts experience a certain degree of randomness due to the usual slip of the rolling elements and the cage. However small this effect might be (a few percent), it is usually enough to exclude the resulting signal from the class of periodic processes. Consequently, it was demonstrated in [6] that a localized bearing fault could be modelled as a *2nd order cyclostationary* process, i.e. a *random* process with a *periodic* autocorrelation function [7]. Because the period of the bursts is not in general commensurate with that of the modulations, the signal is strictly speaking a *quasi-cyclostationary* process, i.e., one whose autocorrelation function has no finite period but can still be expanded into a sum of Fourier series (i.e., it contains only discrete frequency components).

Additive and Multiplicative Interactions

In the simplest case the participation of bearing and gear vibrations is additive. Separation of the two signals can thus be achieved on this basis, for instance by using synchronous averaging or the Self-Adaptive Noise Cancellation (SANC) principle [8]. Experiments on the UNSW test-rig have clearly supported this point. One of the bearings (Koyo 1250, double row self-aligning) supporting the gears was purposely damaged by machining a small slot in its outer race. Figure 2 displays the measured accelerometer signal. 20 synchronous averages were performed to extract the periodic part, shown in Fig. 2(*b*), and the residual part in Fig. 2(*c*). As can be seen, the extracted periodic part pertains mainly to gear vibrations, whereas the residual part—which is 2nd order cyclostationary—essentially pertains to the bearing fault; small impacts appear with a periodicity approximately equal to the ball-pass period. Similar experiments showed that a gear fault and a bearing fault occurring in the same signal could be well separated in the same way.

However, cases have been encountered where the relationship between the gear and bearing signals is largely multiplicative, meaning that the separation may not be as straightforward. This may occur, for instance, because the force at the gear mesh is reacted at the bearings, and changes in the support given by the bearings (e.g., due to some defect), cause a modulation of the gear mesh signal. However, a careful analysis of this case shows that the signal can still be decomposed into a periodic and a 2nd order cyclostationary component, the latter containing the information on possible bearing faults [9].

Stochastic Models for Bearing Faults

This section gives a better basis for the previous discussion by introducing an analytical model for the generating process of a fault in a rolling element bearing. Having a simple model that can reproduce the vibration signals to a sufficient degree of accuracy is important for many reasons. First, the effort put into modelling undeniably leads to a better understanding of the signal to be analyzed. Second, it helps in formalizing existing techniques. Finally, it can lead to the design of specific analysis and diagnostic tools.

Two cases are considered here. The first one relates to localized faults where the generating process is a train of pulses corresponding to the impacts on the defect. The second one is for distributed faults, where the generating process is a modulated random noise.

1 Localized Faults. A comprehensive model for the vibration signal produced by a localized defect in rolling element bearings was proposed by McFadden [10]. That model explicitly incorporated the nonstationarity of the vibration signal by including different sources of amplitude modulations. The model was later refined by D. Ho, by taking into account the random period fluctuations which are likely to occur in the real world [11].

Specifically, let us denote by $F(t)$ the impacting force process, by A_i the amplitude of the i^{th} impact on the defect and by T_i its time of occurrence. Then

$$F(t)=\sum_i A_i\delta(t-T_i) \tag{1}$$

where $\delta(t)$ is the Dirac delta function. This equation is to be further convolved with the impulse response of the system to give the vibration signal. In addition, all modulations are embedded in the statistical properties of process A_i (shaft or cage modulation as discussed above). Figure 3 gives a schematic representation of $F(t)$ along with the vibration signal it might produce.

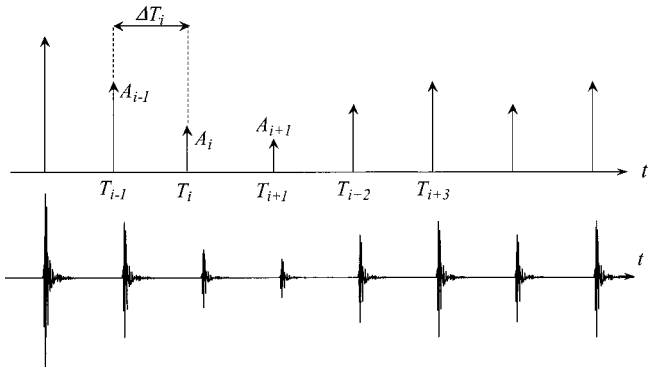

Fig. 3 The impacting process and the corresponding expected vibration signal (e.g., acceleration)

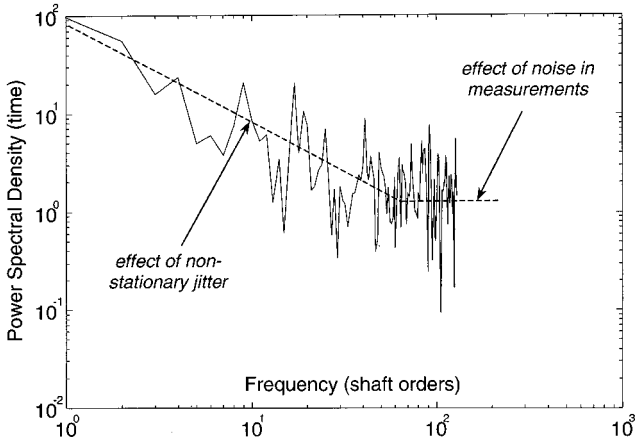

Fig. 4 Power spectral density of the time jitter process ($T_i - iT$) measured on an actual rolling element bearing (inner race fault)

In [6], it was supposed that the times of occurrence were fixed on a periodic grid with a given spacing T, but with some random *jitter* around each node so that

$$T_i = iT + \delta T_i \tag{2}$$

where iT is the expected i^{th} time of occurrence and δT_i the random uncertainty around it (typically a few percent of T). This gave a conditional probability of occurrence,

$$P[T_i = t_i | T_j = t_j] = P[T_i = t_i] \quad j < i \tag{3}$$

that is, the probability was only conditioned by the fact that T_i had to fall close to the i^{th} node of a predefined grid, whatever the times of occurrence of the previous impacts. This model would have certainly been valid if the cage speed were a fixed proportion of the shaft speed, so that the randomness came only from variations in rolling element spacing in the cage. However, the position and thus the speed of the cage is directly affected by slip of the rolling elements, and once it has departed from its kinematic position (no slip) there is no reason why this slip should be corrected in order to make the mean speed constant.

Thus, another more likely mechanism is that an impact falls about T seconds later than the previous one, whatever the actual time of occurrence of the previous one. In mathematical terms, the conditional probability for the occurrence of the i^{th} impact would be

$$P[T_i = t_i | T_j = t_j] = P[T_{i-j} = t_i - t_j] \quad j < i \tag{4}$$

This allows for cage slip in bearings with respect to the kinematic cage position. Incidentally, this second model leads to completely different statistical properties, though the time traces of the impacting forces look very similar. We define ΔT_i as the inter-arrival times between two adjacent impacts, i.e. $\Delta T_i = T_i - T_{i-1}$. Basically, the main difference between the two models is that the former is defined by the mutual independence of the jitter δT_i whereas the latter is defined by the mutual independence of the inter-arrival time ΔT_i.

Both models can be shown to have the same expected value $E[T_i] = iT$, but their covariance functions are respectively

$$Cov[T_i, T_j] = \sigma_\delta^2 \delta_{ij} \tag{5}$$

and

$$Cov[T_i, T_j] = \min(i,j)\sigma_\Delta^2 \tag{6}$$

with σ_δ and σ_Δ the standard deviation of δT_i and ΔT_i. From these results, the first model is recognized as producing a *wide sense stationary* jitter process $T_i - iT$, whereas the second model causes it to be *nonstationary*. In the second model, the time jitter $T_i - iT$ is actually a *random walk*, i.e. the discrete version of *Brownian motion*.

As an example, Fig. 4 displays the spectrum of the jitter process measured on an actual faulty rolling-element-bearing with an inner race fault. It is made up of two parts, the first part (slope -1) clearly pertaining to the nonstationary jitter effect (Eq. 4), and the second (horizontal slope) probably due to additive noise.

The important implication from distinguishing the two types of random jitter is the following. The impacting process as given by Eq. (1) is only cyclostationary under Eq. (3), i.e., it has a periodic autocorrelation function $R_{FF}(t,\tau)$, such that [7],

$$R_{FF}(t,\tau) = E\left\{ F\left(t - \frac{\tau}{2}\right) F\left(t + \frac{\tau}{2}\right) \right\} = R_{FF}(t+T,\tau) \tag{7}$$

As a consequence, the resulting vibration signal will also be cyclostationary. On the other hand, Eq. (4) yields an autocorrelation function which gradually dies to some constant value:

$$\lim_{t \to \infty} R_{FF}(t,\tau) = C < \infty \tag{8}$$

The departure from cyclostationarity may actually be extremely slow, especially if the random fluctuations are small (σ_Δ less than a few percent of T). Under this condition, it is convenient to assume cyclostationarity as a first approximation. We shall refer to such processes as *pseudo-cyclostationary* processes, as they appear to be cyclostationary but actually are not. This is by analogy with pseudo-random signals which appear to be random, but are actually periodic.

Figure 5 illustrates the typical power spectrum as generated by a cyclostationary impacting process (constant amplitude) simulated from Eq. (3). Figure 6 illustrates the pseudo-cyclostationary impacting process from Eq. (4). Note the smearing of the peaks due to the nonstationarity of the inter-arrival times for the pseudo-cyclostationary process. Of importance though is the fact that the two spectra are superimposed *on a broadband continuous density*,

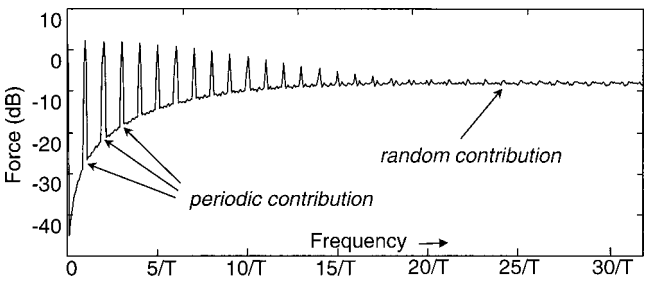

Fig. 5 Power spectrum of the cyclostationary impacting process $F(t)$ with $\sigma_\delta = T/100$

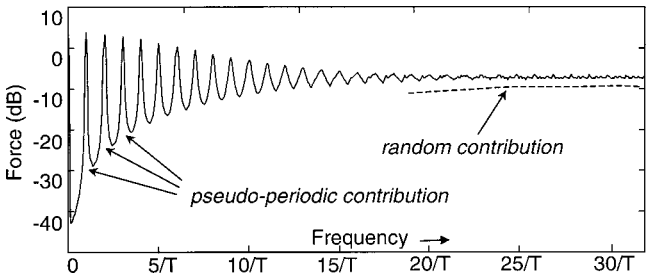

Fig. 6 Power spectrum of the pseudo-cyclostationary impacting process $F(t)$ with $\sigma_\Delta = T/50$

due to the random nature of the time jitter process. It is this continuous background that really makes the difference with a periodic process as would be the case for example for a cracked tooth in a gear signal.

2 Distributed Faults. Usually, a localized defect rapidly propagates on the surface where it was initiated or, by contamination, on contacting surfaces. At more advanced stages, the defect may have spread over a large area and become smoothed out. Such cases are typical of extended spalling on the inner or outer race. The vibration signal produced by a distributed fault is no longer impulsive, but rather has a randomly distributed phase, for the rolling elements are on a different position on the rough surface for every revolution. When the fault is on the inner race, it periodically enters and exits the load zone and the resulting signal is modulated by the shaft speed. This again defines a cyclostationary process. Note that, for a distributed fault, the notion of random time jitter is meaningless and the process is purely cyclostationary (as opposed to pseudo-cyclostationary). Moreover, when the fault only extends over a limited sector of the race, strong periodic components are generated at the shaft periodicity and the bearing fault signal may be written:

$$X_b(t) = p(t) + B(t)$$
$$E[B(t)] = 0 \tag{9}$$

where $p(t)$ accounts for the periodic component and $B(t)$ for the purely random—but cyclostationary—component. If only $p(t)$ is analyzed, the fault could incorrectly be diagnosed as a gear fault, since it gives the same pattern of frequencies. However, analysis of $B(t)$ would differentiate the two situations as it is theoretically zero in a gear signal. Figure 7 illustrates a typical power spectrum as expected from a distributed fault. Note the presence of a continuous background spectrum associated with $B(t)$, which would not exist for a gear fault. This is in perfect accordance with the previous conclusion on localized faults.

Fault Detection Schemes

The previous sections have demonstrated that the vibration signal induced by bearing faults is suitably typified as *cyclostationary* or *pseudo-cyclostationary*, as opposed to *periodic* for gears. This is irrespective of the distribution of the fault, whether it is localized or spread. This suggests using cyclostationarity as a means of detecting bearing faults, and differentiating them from gear faults if need be.

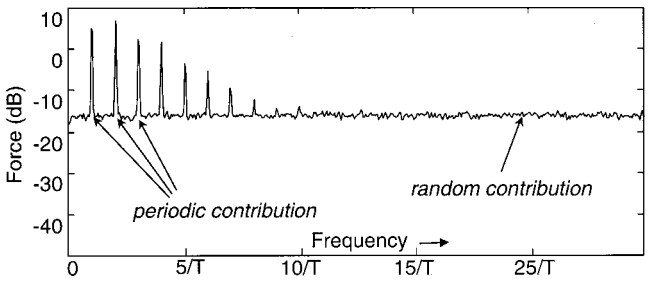

Fig. 7 Power spectrum of the generating process $F(t)$ of a distributed fault

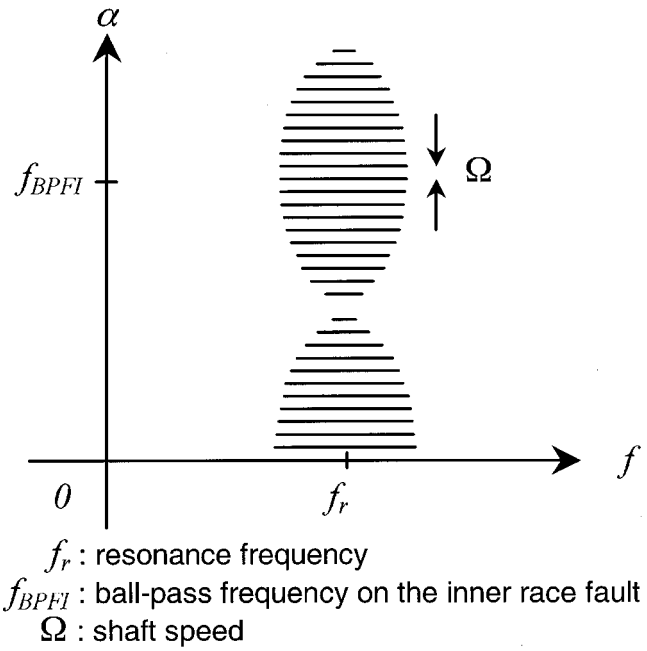

Fig. 8 Spectral correlation density of a localized inner race fault

An efficient method for testing cyclostationarity of a signal $X(t)$ is to compute the two-dimensional Fourier transform of its autocorrelation function $R_{xx}(t,\tau)$, i.e.

$$S_{xx}(\alpha, f) = \underset{\substack{t\to\alpha \\ \tau\to f}}{F}\{R_{xx}(t,\tau)\} \tag{10}$$

The bivariate function $S_{xx}(\alpha, f)$ is known as the *spectral correlation* density. Since for a cyclostationary signal the autocorrelation function is periodic in the variable t while being transient in the variable τ, the spectral correlation density gives rise to a family of parallel spectra, *continuous* in the f frequency, but *discretely distributed* in the α direction—with a slight smearing as in Fig. 6 if the signal is in fact pseudo-cyclostationary. On the other hand, for stationary signals (no variations with t), only the spectrum at $\alpha = 0$ has non-zero values in the f direction, this actually being the power spectral density. Finally, for purely periodic signals, the spectral correlation density is not continuous but discrete both in the α and f direction, thus being made up of a "bed of nails."

Therefore, a simple test for evidence of cyclostationarity is based on checking for continuity of the spectral correlation density for some values of $\alpha \neq 0$. According to the distribution of the fault, different strategies may be devised.

1 Detection of Localized Faults. Figure 8 shows schematically the expected spectral correlation density in case of a localized fault—e.g., on the inner race. The spectral correlation density is typically concentrated around some resonance frequency f_r in the f direction, and centered on the ball-pass frequency on the fault (f_{BPFI}) in the α direction [6]. For an inner race fault, this would be further quantized with low harmonics and sidebands with spacing corresponding to the shaft speed Ω. The expected shape is in accordance with that of a (quasi-) cyclostationary process, i.e., discrete over α and continuous over f.

In some complex systems, the harmonics of the gearmesh frequencies would possibly extend over the excited resonance fre-

quency f_r. Then a whole pattern of equi-spaced points as schemed in Fig. 10 would superpose with the spectral density of Fig. 8. These could however be removed by application of the SANC as proposed in [8,11].

Reference [6] pointed out how cumbersome it is to compute the 2-D spectral correlation density in practical applications. It was shown therein that the integration of the spectral correlation density over the f direction gives the most important diagnostic information for discrete faults. This procedure was shown to result in a discrete spectrum in the α variable, which actually compares with the classical Envelope Spectrum [5], for it is simply the Fourier transform of the *mean squared* signal (i.e., the spectrum of the squared envelope).

2 Detection of Distributed Faults. In the case of distributed faults, the spectral correlation density is somewhat different. For an outer race fault, it is only continuous for $\alpha=0$ and thus does not help in detecting it. For an inner race fault, it is continuous for α equal to the shaft rotation frequency and possibly some of its harmonics. Finally, for a ball fault, it is continuous for α equal to the cage rotation frequency.

It was previously pointed out that in gearboxes, distributed bearing faults are likely to modulate the gearmesh frequencies. The resulting spectral correlation density would then have an intricate pattern, where all the discrete peaks of the gear signal carry the aforementioned continuous spectral lines due to $B(t)$ in Eq. (9) and possibly discrete peaks due to $p(t)$ in Eq. (9). This is illustrated in Fig. 9 in case of an inner race fault, where f_0 stands for the gearmesh frequency and Ω for the shaft speed. Note the presence of the discrete side-bands around each gearmesh harmonic—spaced by the shaft speed—which are responsible for the diamond shape.

Indeed, the spectral correlation density of a distributed bearing fault closely resembles that of a gear signal, as exemplified in Fig. 10.

The only difference lies in the presence of continuous ''horizontal'' spectra for all

$$\alpha = f_0(p-q) - k\Omega, \quad p,q = 1,2,\ldots \quad k = 0,\pm 1,\pm 2,\ldots \tag{11}$$

and centered on all

$$f = f_0(p+q)/2 \quad p,q = 1,2,\ldots \tag{12}$$

Just as before, it is specifically these spectral lines which would give evidence of a bearing fault, along with its characteristic frequency. However, caution should be taken when integrating the spectral correlation density—or equivalently computing the squared-envelope spectrum—as was suggested above for localized faults, because the resulting spectrum could not differentiate between gear and bearing faults. As a matter of fact, projection of Fig. 9 or Fig. 10 onto the α axis ends up with the same result, with some scaling factor. Before resorting to the squared-envelope spectrum, it is therefore desirable to first remove the periodic components in the signal, for instance by synchronous averaging or with the SANC [8].

Another alternative to the integrated or squared-envelope spectrum is to analyze the spectral correlation density as a function of f, for a given α. For example if the vibration signal is to be checked for an inner race fault, then any value of α as given in Eq. (11) could be used. If the resulting spectrum has a continuous part, then it indicates a bearing fault. Otherwise it is purely discrete because of the gearmesh carriers and shaft side-bands.

For illustration, a typical vibration signal from a single-stage gearbox was simulated by amplitude modulating a gearmesh frequency with 6 harmonics. Some white noise was also added to produce a realistic signal-to-noise ratio of 14 dB. Figure 11 dis-

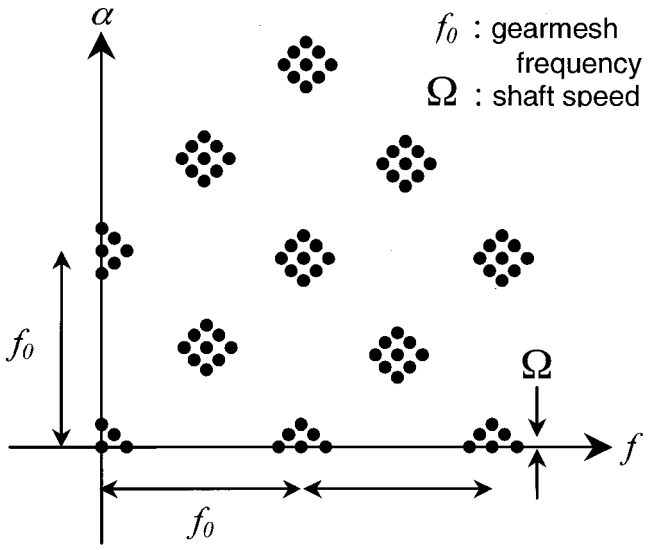

Fig. 10 Spectral correlation density of a gear signal

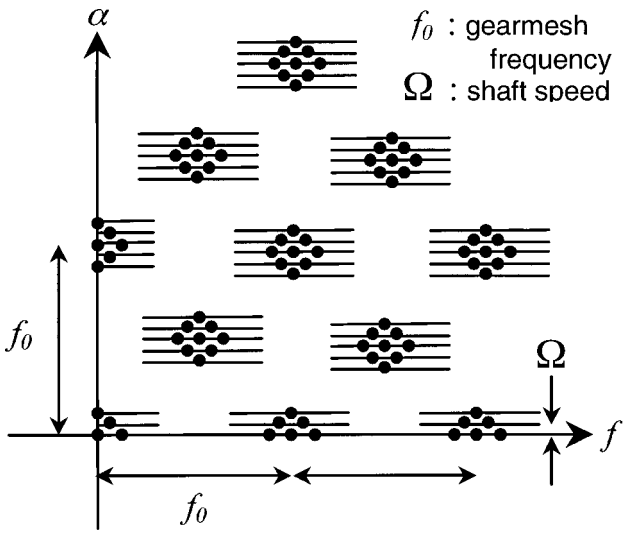

Fig. 9 Spectral correlation density of an advanced inner race fault

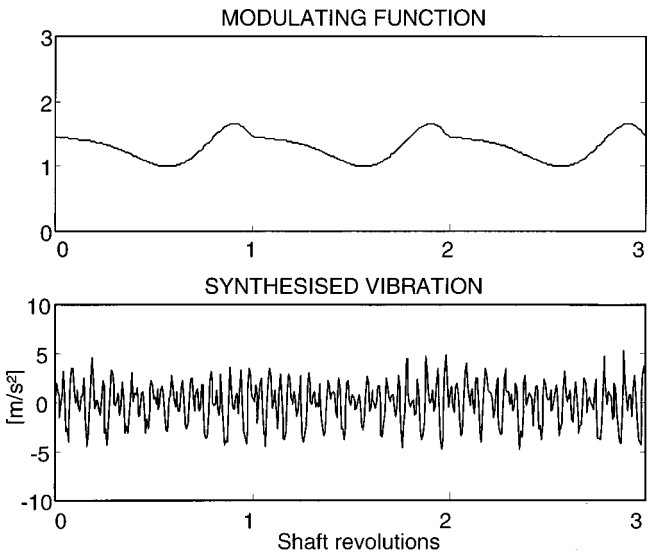

Fig. 11 Simulated gear signal

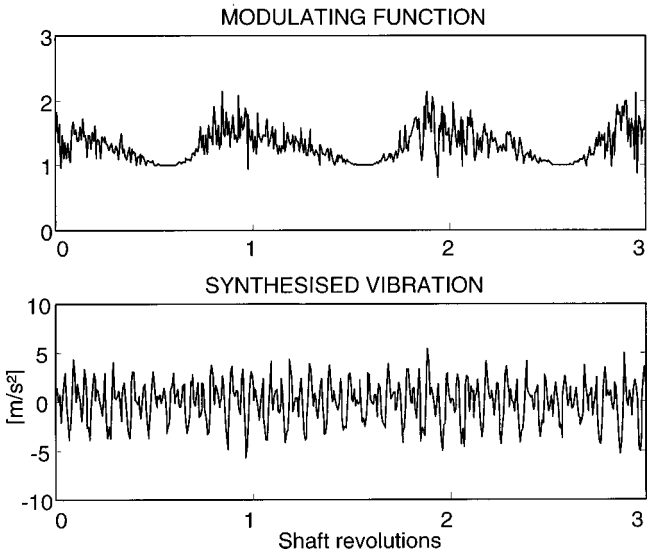

Fig. 12 Simulated gear signal modulated by an advanced inner race fault

plays the vibration signal where only the modulation from the gear is present. Figure 12 displays the expected signal when an advanced spalled inner race defect has occurred. As can be seen from these figures, the two vibration signals are barely distinguishable in spite of the modulating functions being rather different.

Indeed, if only the spectral line $\alpha=0$ were considered as in classical spectral analysis, it would be impossible to distinguish the two cases. A bearing fault would indeed increase the overall *continuous* level of the power spectrum—due to the cyclostationary part at $\alpha=0$, but this could just as well be attributed to an increase in the stationary background noise. On the other hand, if some other spectral lines as given by Eq. (11) ($\alpha\neq 0$) are considered, an increase in the spectrum is necessarily due to a cyclostationary component.

This is illustrated in Fig. 13 and 14, which compare the spectral correlation density taken for $\alpha=\Omega$ (shaft speed) before and after the occurrence of the bearing fault. The obvious increase of 25 dB in Fig. 14 does necessarily come from a cyclostationary process and thus can be assigned to a bearing fault.

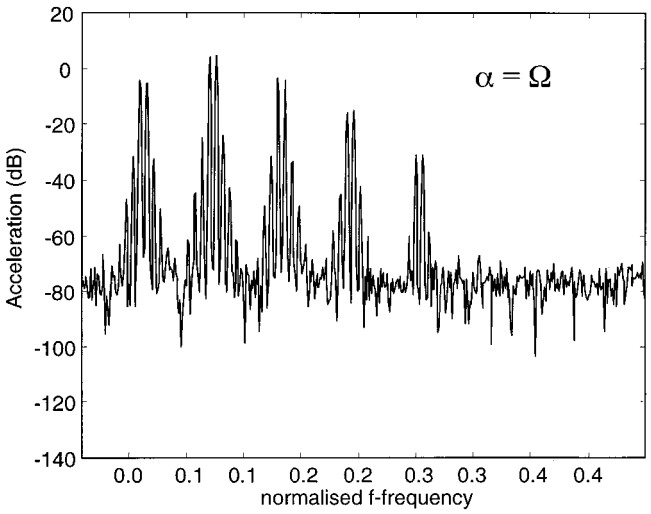

Fig. 13 Spectral correlation density for $\alpha=\Omega$ in the fault-free case

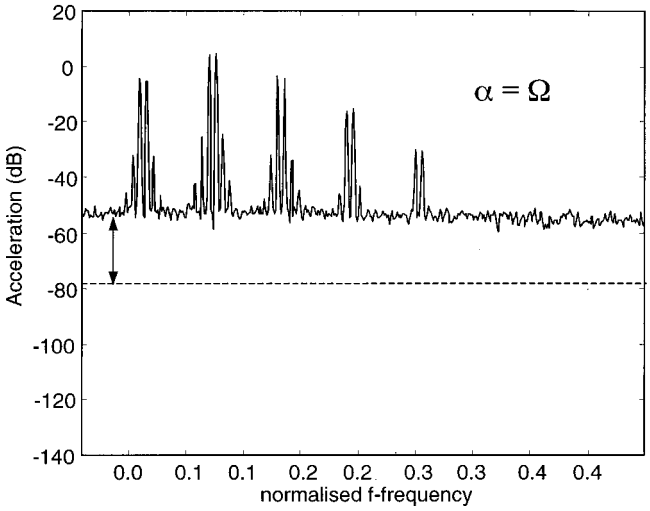

Fig. 14 Spectral correlation density for $\alpha=\Omega$ in the faulty case

The proposed diagnostic procedure was tested on the UNSW test-rig. Two wheels with a speed increase ratio of 49:32 were assembled and a rough surface was ground over half of the inner raceway of the bearing supporting the output shaft. The vibration signal was measured before and after the insertion of the bearing fault, and the periodic components were removed by the SANC. It was actually observed that the healthy signal was almost perfectly periodic, whereas the faulty signal experienced a lot of randomness. Figure 15 displays the spectral correlation densities of the residual signals for $\alpha=\Omega$ (output shaft speed). The faulty signal shows a dramatic increase in power at this cyclic frequency (up to 40 dB), hence clearly indicating a cyclostationary fault. Closer inspection of the spectra revealed that the bearing fault manifested itself as multiplicative, since it mainly modulated the gearmesh harmonics in the range of order up to 700.

Other experiments were able to verify that the proposed procedure also applied to localized faults. Here the test-rig was equipped with a 1:1 ratio and a slot machined on the inner race of the bearing supporting the input shaft. Figure 16 displays the spectral correlation densities at $\alpha=\Omega$ for the good and faulty cases. Manifestation of cyclostationarity is again clearly evi-

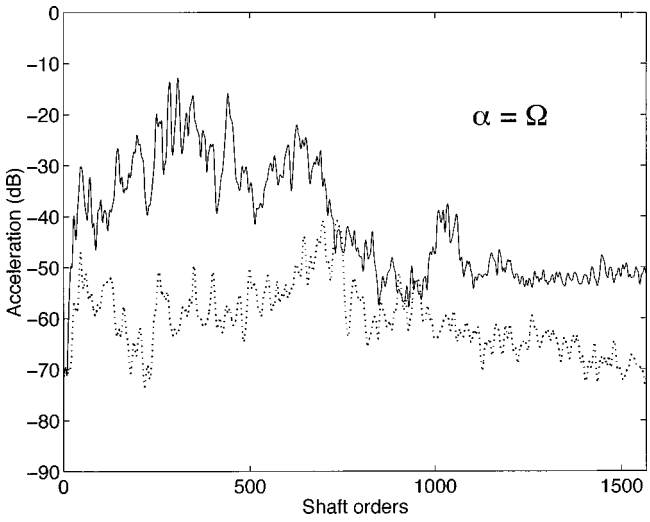

Fig. 15 Spectral correlation density for $\alpha=\Omega$: dotted line—healthy case; continuous line-rough surface on half the inner race. Tracking on the output shaft.

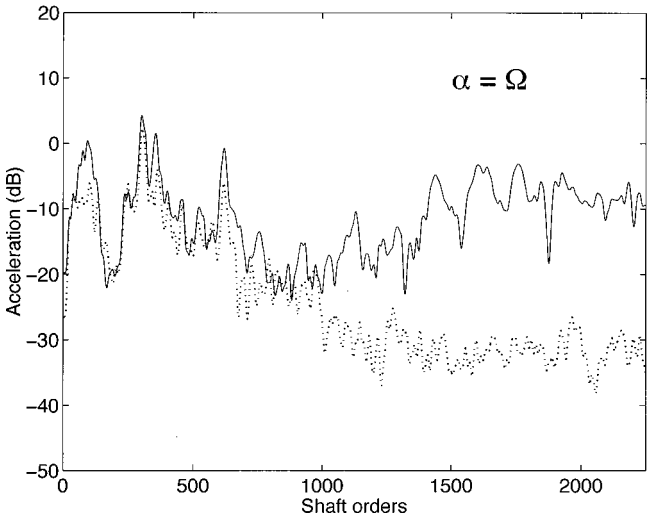

Fig. 16 Spectral correlation density for $\alpha=\Omega$: dotted line—healthy case; continuous line-slot on the inner race. Tracking on the input shaft.

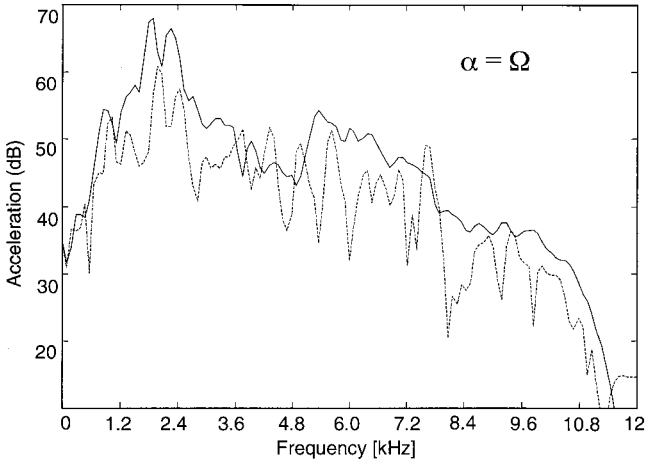

Fig. 17 Spectral correlation density for $\alpha=\Omega$: dotted line—healthy case; continuous line-inner race fault

denced. The bearing fault was checked to be mainly additive since it appeared well above the significant gearmesh harmonics. In this case envelope analysis also gave excellent results in the high frequency range

The next example is taken from an actual gearbox from a Sea Hawk Helicopter SH-60, where evidence of a distributed bearing inner race fault was reported. Although some extra amplitude modulation was apparent on the time signals, it was difficult to relate it either to a bearing or a gear fault. Indeed, the power spectral densities in the fault-free and the faulty cases were almost identical. Figure 17 shows the spectral correlation density taken for $\alpha=\Omega$, where again the presence of a bearing fault is clearly evidenced by an overall increase in power.

Conclusion

This paper investigated how to differentiate bearing from gear faults through the analysis of their vibration signals. The key idea is to recognize bearing fault signals as cyclostationary, as opposed to periodic for gears. A comprehensive analysis of bearing faults was conducted in terms of the type of cyclostationarity they induce. Distinction was made between localized and distributed faults.

For localized faults, a further distinction opposed stationary to nonstationary time jitter in the impacting process. It was demonstrated that the latter case produces a pseudo-cyclostationary vibration signal, which can however be treated as cyclostationary in a first approximation.

For distributed faults, the discussion led to the proposal of a specific diagnostic procedure based on advanced—but simple to use—spectral analysis. The effectiveness of the proposed procedure was checked on experimental and actual vibration signals from gearboxes.

References

[1] Burchill, R. F., Frarey, J. L., and Wilson, D. S., 1973, "New Machinery Health Diagnostic Techniques Using High-Frequency Vibration," SAE paper 730930.
[2] Randall, R. B., 1982, "A New Method of Modeling Gear Faults," J. Mech. Des., **104**, pp. 259–267.
[3] McFadden, P. D., 1986, "Detecting Fatigue Cracks in Gears by Amplitude and Phase Demodulation of the Meshing Vibration," ASME J. Vibr. Acoust., **108**, pp. 165–170.
[4] Dyer, D., and Stewart, R. M., 1978, "Detection of Rolling Element Bearing Damage by Statistical Vibration Analysis," J. Mech. Des., **100**, pp. 229–235.
[5] McFadden, P. D., and Smith, J. D., 1984, "Vibration Monitoring of Rolling Element Bearings by the High Frequency Resonance Technique—A Review," Tribol. Int., **117**, No. 1, pp. 3–10.
[6] Randall, R. B., and Antoni, J., 2001, "The Relationship between Spectral Correlation and Envelope Analysis in the Diagnostics of Bearing Faults and other Cyclostationary Machine Signals," Mech. Syst. Signal Process., **15**, No. 5, pp. 945–962.
[7] Gardner, W. A., 1986, *Introduction to Random Processes With Applications to Signals and Systems*, Macmillan.
[8] Antoni, J., and Randall, R. B., 2001, "Optimization of SANC for Separating Gear and Bearing Signals," *Condition Monitoring and Diagnosis Engineering Management Conference*, Manchester, UK, pp. 89–96.
[9] Randall, R. B., and Antoni, J., 2001, "Separation of Gear and Bearing Fault Signals in Helicopter Gearboxes," *Acoustical and Vibratory Surveillance Methods and Diagnostic Techniques*, 16–18 Oct., Compiègne, FR, pp. 161–183.
[10] McFadden, P. D., and Smith, J. D., 1984, "Model for the Vibration Produced by a Single Point Defect in a Rolling Element Bearing," J. Sound Vib., **96**, No. 1, pp. 69–82.
[11] Ho, D., and Randall, R. B., 2000, "Optimization of Bearing Diagnostic Techniques Using Simulated and Actual Bearing Fault Signals," Mech. Syst. Signal Process., **14**, No. 5, pp. 763–788.